Title: Homozygous loss-of-Function mutations in *SLC26A7* cause goitrous Congenital Hypothyroidism

Supplementary Appendix

Contents

Page	Section
2	Methods including Supplementary Table 1 (p4)
12	References
14	Figures
17	Clinical Tables (Supplementary Tables 2, 3)

Authors: H Cangul*[1], X-H Liao*[2], E Schoenmakers[3], J Kero[4, 5], S Barone[6], P Srichomkwun[2], H Iwayama[2], E.G Serra[7], H Saglam[8], E Eren[8], O Tarim[8], A.K Nicholas[3], I Zvetkova[3], C.A Anderson[7], F.E Karet Frankl[9], K Boelaert[10], M Ojaniemi[11], J Jääskeläinen[12], K Patyra[4], C Löf[4], E.D Williams[13], UK10K Consortium, M Soleimani[6], T Barrett[14], E.R Maher[15], V.K Chatterjee[3], S Refetoff[2,16], N Schoenmakers**[3]**

*These authors contributed equally

** Coequal corresponding authors

Supplementary Methods

Whole-Exome Sequencing

Whole-exome sequencing was performed on two siblings with congenital hypothroidism (CH) (AII.i and AII.iii)), as part of the UK10K project. Previous studies had not demonstrated linkage to known CH-associated genes in these two subjects. DNA (1-3 mg) was sheared to 100-400 bp fragments using a Covaris E210 or LE220 (Covaris). Sheared DNA was subjected to Illumina paired-end DNA library preparation and enriched for target sequences (Agilent Technologies; Human All Exon 50 Mb - ELID S02972011) according to manufacturer's recommendations (Agilent; SureSelectXT Automated Target Enrichment for Illumina Paired-End Multiplexed Sequencing). Enriched libraries were sequenced using the HiSeq platform (Illumina) as paired-end 75 base reads according to manufacturer's protocol. The Burrows-Wheeler Aligner (Li and Durbin, 2009) was used for alignment to the human reference genome build UCSC hg19 (Grch37). To improve raw alignment BAMs for SNP calling, we realigned around known (1000 Genomes pilot) indels and recalibrated base quality scores using GATK (DePristo et al., 2011). Base alignment quality tags were added using SAMtools calmd. BAMs for each sample were merged and duplicates marked using Picard. Variants (SNVs and indels) were called on each sample individually with both SAMtools mpileup (0.1.17) (Li et al., 2009) and GATK Unified Genotyper (1.3.21) (McKenna et al., 2010), restricted to exon bait regions plus or minus a 100 bp window. Various quality filters were applied to each of the callsets separately, following current best practices. Calls were then merged, giving preference to GATK information when possible. Calls were annotated with 1000 Genomes allele frequencies phase I integrated call set, dbSNP137 rsids, and earliest appearance in dbSNP. Functional annotation was added using

Ensembl Variant Effect Predictor v2.8 against Ensembl 70 and included coding consequence predictions, SIFT, PolyPhen and Condel annotations, and GERP and Grantham Matrix scores.

We analyzed non-synonymous coding, nonsense, and splice-site variants, which were thought more likely to be pathogenic than intronic, 5'- and 3'-UTR variants. Given the consanguineous background, we focused on shared, homozygous variants and filtered against dbSNP to retrieve novel variants or variants with minor allele frequency <1% which were unique to the Thyroid disease cohort within the UK10K project. This filtering approach identified 4 novel homozygous variants (Supplementary Table 1), of which only 1 (SLC26A7, p.R227*) was thought to be a biologically likely candidate. There are no homozygous individuals at this site across population databases (including ExAC and gnomAD datasets), with only 6 heterozygous samples (out of 122,598) in gnomAD (a frequency which is consistent with recessive disease, AF = 0.0002447). Other CH cases were then investigated for mutations in SLC26A7, using WES (Families D and E) or direct sequencing (Families B, C and F). Variants listed in this study are described using the systematic nomenclature approved by the Human Genome Variation Society (HGVS; www.hgvs.org/mutnomen). Nucleotide numbering starts from the A (+1) of the translation initiation codon (ATG) of the NCBI reference sequence NM_052832.3 (ENST00000276609.7). Amino acid residues are numbered according to the NCBI reference sequence NP_439897.

Supplementary Table 1: Rare, Shared Homozygous Variants Identified in AII.i and AII.iii which are predicted to be Pathogenic

Gene	Amino acid change	GERP Score	Polyphen prediction	SIFT prediction	Condel prediction	Comment
ZNF778	S280P	2.52	Possibly_ damaging (0.545)	Deleterious (0.01)	Deleterious (0.591)	Haploinsufficiency associated with intellectual disability, skeletal anomalies
MC1R	V265I	-4.44	Benign (0.126)	Deleterious (0.04)	Neutral (0.359)	MSH receptor
DDX53	K325E	2.25	Benign (0.281)	Deleterious (0.03)	Neutral (0.451)	Contains domains found in DEAD-box helicase proteins (participate in ATP-dependent RNA unwinding)
SLC26A7	**R227***	**0.94**	**.**	**.**	**.**	**Anion channel, same family as Pendrin, most likely candidate for CH**

Sanger Sequencing of *SLC26A7*

The DNA template of the SLC26A7 gene was downloaded from the Ensembl database (ENSG00000147606). All alternative protein coding transcripts (5 in total) were included to ensure that primers were designed to cover all coding exons and intron/exon boundaries. Intronic primers flanking the coding sequence were designed for PCR amplification using ExonPrimer and Primer3. Primer sequences and PCR conditions are available upon request. PCR products were size-checked on 1% horizontal agarose gels and cleaned up using MicroCLEAN (Microzone, Haywards Heath, UK) or QIAquickTM Gel Extraction kit (Qiagen, Crawley, UK). The purified PCR products were sequenced in both forward and reverse directions using the ABI BigDye Terminator v3.1 Cycle Sequencing kits on an ABI Prism 3730 DNA Analyzer (Applied Biosystems, Warrington, UK). Analysed sequences were then downloaded using Chromas software and assessed for the presence of alterations.

Human clinical phenotyping

Biochemistry was measured using local automated assays and local reference ranges.

Perchlorate Tests were performed according to local protocol. AII.i, AII.iii: 10MBq ^{123}I-Na was injected and imaging commenced 2 hours later. 10mg/kg oral sodium perchlorate was then administered, and a second dynamic acquisition acquired 30mins later. CI.i 1 g potassium perchlorate was administered 2 h after a tracer dose of ^{131}I. Thyroidal radioactive iodine uptake was measured immediately before perchlorate administration and at 15 min intervals for 2 hours thereafter. BII.i; Images were acquired 30 minutes after 10MBq ^{123}I-Na injection as a 30 minute dynamic acquisition. Sodium Perchlorate (dose as per Paediatric BNF guidelines) was injected 10 minutes after commencement and discharge assessed at 30mins.

The percentage discharge of iodine from the thyroid gland was calculated using the following

formula:

$$\frac{(\text{uptake before perchlorate} - \text{uptake after perchlorate})}{\text{uptake before perchlorate}} * 100$$

Construction of Expression vectors.

Receptor mutations were generated by site directed mutagenesis of wild type (WT) human SLC26A7 cDNA and cloned into a eukaryotic expression vector (pcDNA3) downstream of a Flag epitope tag (Agostini *et al* 2006) for iodide efflux assays, or with a GFP tag (pEGFP-N3, Clontech) for cell localization assays. Human SLC5A5 with a HA tag in a pcDNA3 vector was a kind gift from Dr N Carrasco, Department of Cellular and Molecular Physiology, Yale School of Medicine, New Haven, Connecticut. SLC26A4 cloned into the expression vector pIRES-EYFP was a kind gift from Dr L Persani Department of Clinical Sciences and Community Health, University of Milan; Division of Endocrinology and Metabolism, IRCCS Istituto Auxologico Italiano, Milan, Italy (Cirello *et al* 2012).

Cell localization assays

HEK293 cells were cultured on glass coverslips in 6 well plates in DMEM/10% FBS/1% PSF and transfected with 0.5ug SLC26A7-GFP construct or GFP expression vector, using lipofectamine, as per the manufacturers protocol. After 24 hours, the medium was refreshed and the cells transferred to a live cell imaging chamber. Cell localization of GFP constructs was visualized using a confocal fluorescence microscope (Zeiss) with ZEN image analysis software.

Iodide Efflux assay

The assay was performed as described previously (Taylor 2002). HEK293 cells were transfected with Flag epitope-tagged SLC26A7, EYFP-tagged SLC26A4 or empty vector (pcDNA3) as described above. 24 hours after transfection, cells were washed in serum-free DMEM medium and incubated for 1 h in 500µl serum-free medium containing Na [^{125}I] at 5 KBq/ml as the only source of iodide. Cells were then washed in HBSS buffer and then incubated with 500µl HBSS for 0–5 min. HBSS was then removed, the cells were lysed in 500µl lysis buffer (5mM Glycyl-glycine pH 7.8; 15mM MgSO4; 22mM EGTA; 1% triton X100; 1mM DTT) and radioactivity measured using the Wizard 1470 automatic gamma counter (Perkin Elmer). Transfection efficiency was assessed by cotransfection with internal control plasmid BOS-beta-galactosidase (30ng/well).

Quantitative Real-Time PCR analysis of gene expression.

RNA from a human tissue library was purchased from Clontech (636643 Human Total RNA Master Panel II). Murine Tissue RNA was extracted from heart, liver and kidney from 3 wild-type C57/BL6 mice using the RNAeast minikit (Quiagen), or purchased from Clontech (Mouse Thyroid Total RNA 9636674). RNA was reverse transcribed and analysed by Taqman quantitative real-time PCR (qPCR) as described (Agostini et al 2006). The following Taqman probes (Applied Biosystems) were used: Human Slc26A7 (Hs01104163_m1), human cyclophilin, Forward 5'-ACGGCGAGCCCTTGG-3', Reverse 5'-TTTCTGCTGTCTTTGGGACCT-3', Probe FAM-CGCGTCTCCTTTGAGCTGTTTGCA-TAMRA, murine Slc26a7 (Mm00524162_m1) and murine Actb (Mm00607939_s1). The comparative Ct method was used to quantify transcripts and normalize to cyclophilin (human) or Actb (mouse) expression levels.

Variant 2 Human Slc26a7 was quantified using the following primers : Forward 5'-TGGAGTCTCCATGCTTGTTG-3', reverse variant 2 5'-AGATCCAAGTTATCAAACAACAG-3' (Sigma-Aldrich) using SYBR green reagent (Applied Biosystems) with an ABI Prism 7900 sequence detection system (Applied Biosystems). Quantitation was achieved by comparison with standard curves generated using serial dilutions of variant 1 and variant 2 WT Slc26a7 expression vectors.

Immunohistochemistry

Mouse thyroid sections were formalin-fixed, paraffin processed, and sectioned for H&E and IHC studies. IHC of thyroid was performed using anti-FLAG [M2]-Alkaline Phosphatase (Sigma A-9469), 1µg/ml or Mouse IgG1 Isotype Control antibody (Invitrogen 02-6100) in 1% Normal Donkey Serum (NDS, Sigma D-9663) / Dako Wash Buffer (TBS-T, Dako S3006) for 16hr at 4°C. NBT/BCIP Substrate System (Dako K0598) was then applied. Brightfield images were captured using a Zeiss Axioscan Z1 microscope with a Dry 20x 0.8NA objective and analyzed using Halo 2.1 (Indica labs).

Transgenic mice:

***Slc26a7* null mice maintenance**

Slc26a7 null mice were generated as previously described (Xu 2009). Mice were housed in a controlled environment at 22 ± 2 C and 12-h alternating dark and 12-h light cycles. They were fed with a regular rodent diet (PicoLab Rodent Diet 20-5053, which provide iodine 0.97 ppm; St. Louis, MO) and water ad libitum.

ASO Mice (Expressing FLAG-Epitope tagged SLC26A7)

The Slc26a7 locus in AB2.2 AB2.2 ES cells, strain 129S5/SvEvBrd was modified to contain the following features (see figure): Recognition sites for Cre, Flp and φC31 recombinases, AdSA (adenovirus splice acceptor site); cDNA encoding Slc26a7 exons 7 to 19 with C terminal FLAG tag sequence followed by SV40 poly A termination sequence; engrailed 2 SA site linked to IRES (encephalomyocarditis virus (EMCV) internal ribosome entry site) and LacZ sequence followed by SV40 polyA and a selection cassette (pgk promoter, Neo (neomycin), bovine growth hormone poly A signal). The modified ES cells were used to create the ASO 129 mutant mice line expressing FLAG-epitope tagged SLC26A7. The sequence of the targeting vector and the genotyping strategy for the mutant mice are available on demand. Embryos containing the modified Slc26a7 allele were obtained from the Wellcome Trust Sanger Institute, where they were generated.

Schematic of the Slc26a7 Targeted locus in ASO mice

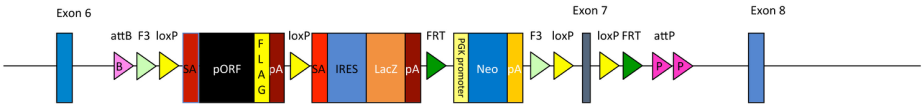

Schematic of the targeted locus: recognition sites for Cre recombinase (loxP yellow triangle), FLP recombinase (FRT green, F3 light green triangles) and φC31 recombinase (attB pink, attP dark pink triangles); Slc26a7 critical exon 7 (grey rectangle); SA - Adeno virus (dark red rectangle) and engrailed 2 splice acceptor (red rectangle) sites, IRES-internal ribosome entry site, pORF- cDNA corresponding to Slc26a7 exon 7 to 19, FLAG - FLAG sequence (yellow rectangle), pA-SV40 - poly A sequences (brown rectangles), LacZ - LacZ sequence, PGK promoter driven Neo cassette and bGH poly A (dark yellow rectangle) sequences. The pORF feature allows the expression of FLAG tagged version of SLC26A7.

Murine Thyroid Hormone Measurement

Murine serum TSH, T4 and T3 measurement has previously been described in detail (Ferrara 2013)

Murine iodide uptake and perchlorate discharge

The ^{125}I uptake and perchlorate discharge tests were performed in accordance with previously described protocols, with minor modifications (Grasberger 2012). In brief, mice aged 60 days were depleted of iodine with a low-iodine diet (Harlan-Teklad, iodine content <0.05 ppm) for 2 weeks and then given a single intraperitoneal (i.p.) injection of ^{125}I (8μCi/mouse). In vivo kinetics of thyroidal ^{125}I accumulation were recorded by counting over the neck with a small probe of the Navigator γ-positioning system (ABS Medical) at different time points over the period of 2 hours. During the perchlorate discharge test, 3 hr after ^{125}I injection, mice were given 10 μg/g body weight $KClO_4$ i.p injection and changes in thyroidal ^{125}I content were monitored. Animals were sacrificed and their thyroid gland dissected 30mins after perchlorate injection. The amount of radioactivity in the thyroid was immediately quantified using a γ-scintillation counter. The amount of radioactivity in thyroid was expressed as fraction of the ^{125}I injected dose for the iodide uptake study, and as a percentage of radioactivity relative to that immediately prior to KClO4 injection in the perchlorate discharge study.

Murine Intrathyroidal TG-bound and Free Thyroid Hormone Measurement.

In order to measure thyroidal TG-bound and free T4 and T3 concentration, mouse thyroid was excised and weighed and hormone content was extracted following the protocol described previously (Di Cosmo 2010)

Murine iodide supplement and serum iodide measurement.

3 Slc26a7 null mice and 3 heterozygous littermates as controls, at P88-P90, were maintained on regular diet with the addition of KI to drinking water at 8µg/ml (equivalent to 30µg iodide/day). Serum was taken to measure thyroid hormone levels at baseline, 2 weeks and 4 weeks, and mice were sacrificed after 6 weeks at P129-131, with further blood sampling for thyroid hormone measurement. Serum iodide concentration was measured at Trace Element Unit, Southampton General Hospital, Southampton UK, by Inductively coupled plasma mass spectrometry using a NexION 300D (Perkin-Elmer Instruments, Beconsfield)

References

Agostini M, et al. Non-DNA binding, dominant negative, human PPARγ mutations cause lipodystrophic insulin resistance. *Cell Metab.*2006*;* 4(4):303-311

Cirello V, et al. Molecular and functional studies of 4 candidate loci in Pendred syndrome and nonsyndromic hearing loss. *Mol Cell Enodcrinol.* 2012;351(2):342-350

DePristo MA, et al. A framework for variation discovery and genotyping using next-generation DNA sequencing data. *Nat. Genet*. 2011;43(5):491–498

Di Cosmo C, et al. Mice deficient in MCT8 reveal a mechanism regulating thyroid hormone secretion. *J Clin Invest*. 2010;120(9): 3377-3388

Ferrara AM, et al. Changes in thyroid status during perinatal development of MCT8-deficient male mice. *Endocrinology* 2013;154(7): 2533-2541

Grasberger H, et al. Mice deficient in dual oxidase maturation factors are severely hypothyroid. *Mol Endocrinol.* 2012;26(3):481-492

Li H, Durbin R. Fast and accurate long-read alignment with Burrows-Wheeler transform *Bioinformatics* 2009;25(14):1754-1760

Li H, et al. 1000 Genome Project Data Processing Subgroup The Sequence Alignment/Map format and SAMtools. *Bioinformatics* 2009;25(16):2078–2079

McKenna A, et al. The Genome Analysis Toolkit: a MapReduce framework for analyzing next-generation DNA sequencing data. *Genome Res*. 2010;20(9):1297–1303

Taylor JP, et al. Mutations of the PDS gene, encoding pendrin, are associated with protein mislocalization and loss of iodide efflux: implications for thyroid dysfunction in Pendred syndrome. *J Clin Endocrinol Metab.* 2002;87(4):1778-1784

Xu, J, et al. Deletion of the chloride transporter slc26a7 causes distal renal tubular acidosis and impairs gastric acid secretion. *J Biol Chem.* 2009;284(43):29470-29479

Supplementary Figure 1: Thyroid hormone levels in Male Heterozygous (A) and Female Homozygous (B) *Slc26a7* null mice compared with wild-type mice and measurement of hormone biosynthetic pathways (iodide uptake, organification) (C, D) in male *Slc26a7* null mice

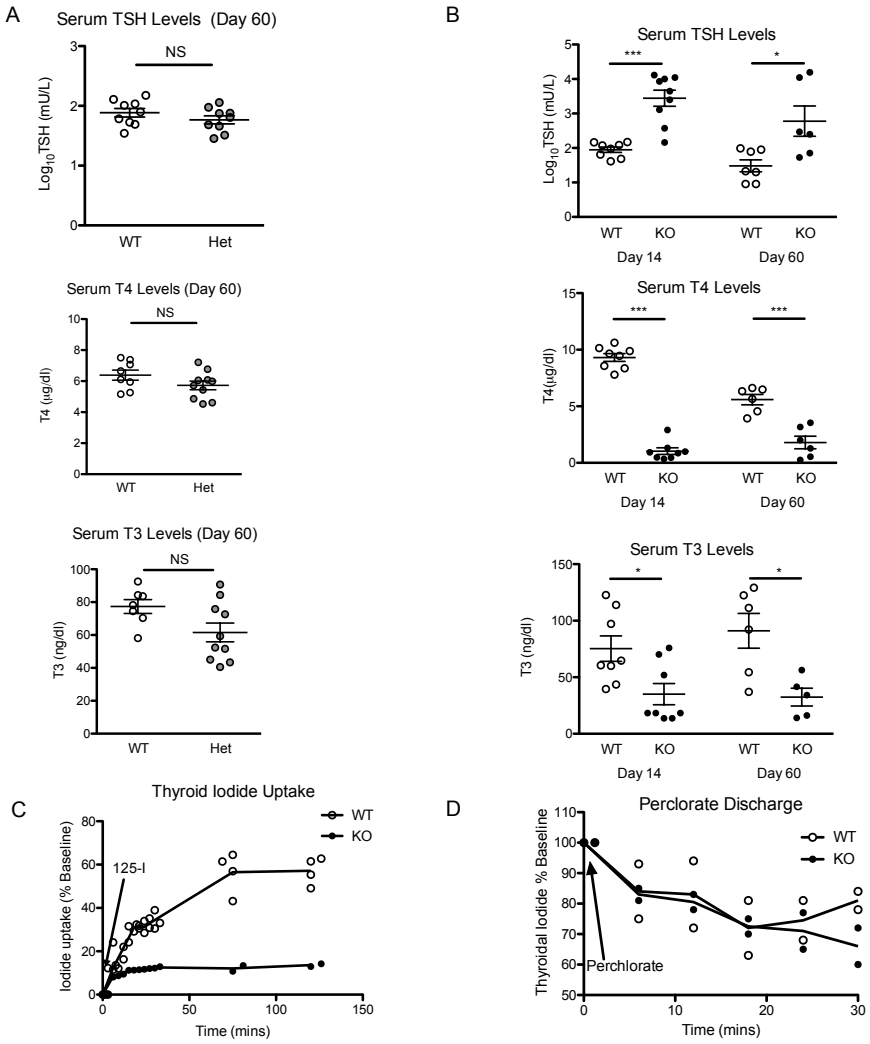

A. Log_{10}TSH, T4 and T3 measurements in male wild-type (white, WT), and heterozygous (Het) Slc26a7 null mice (grey) aged 60 days. Measurements were made from 6-17 mice of each genotype. P values were calculated using an unpaired 2-tailed Student's T-test, horizontal bars represent the mean and error bars represent the standard error of the mean. NS: not significant (P=>0.05) B. Log_{10}TSH, T4 and T3 measurements in female wild-type (WT, white), and Slc26a7 null mice (KO, black) aged 14 and 60 days. Measurements were made from 6-9 mice of each genotype. P values were calculated using an unpaired 2-tailed Student's T-test and horizontal bars represent the mean and error bars represent the standard error of the mean. *P <0.05, **P <0.005, ***P <0.0005. C. Thyroidal iodide uptake and D. discharge of iodide after administration of perchlorate in male *Slc26a7* KO mice compared with wild-type littermates. Measurements were made in 2-4 mice of each genotype aged 90 and 107 days. 125-I (C) and Perchlorate (D) were administered at time=0mins. Lines represent the mean for each group.

Supplementary Figure 2: Representative genotyping data from ASO mice.

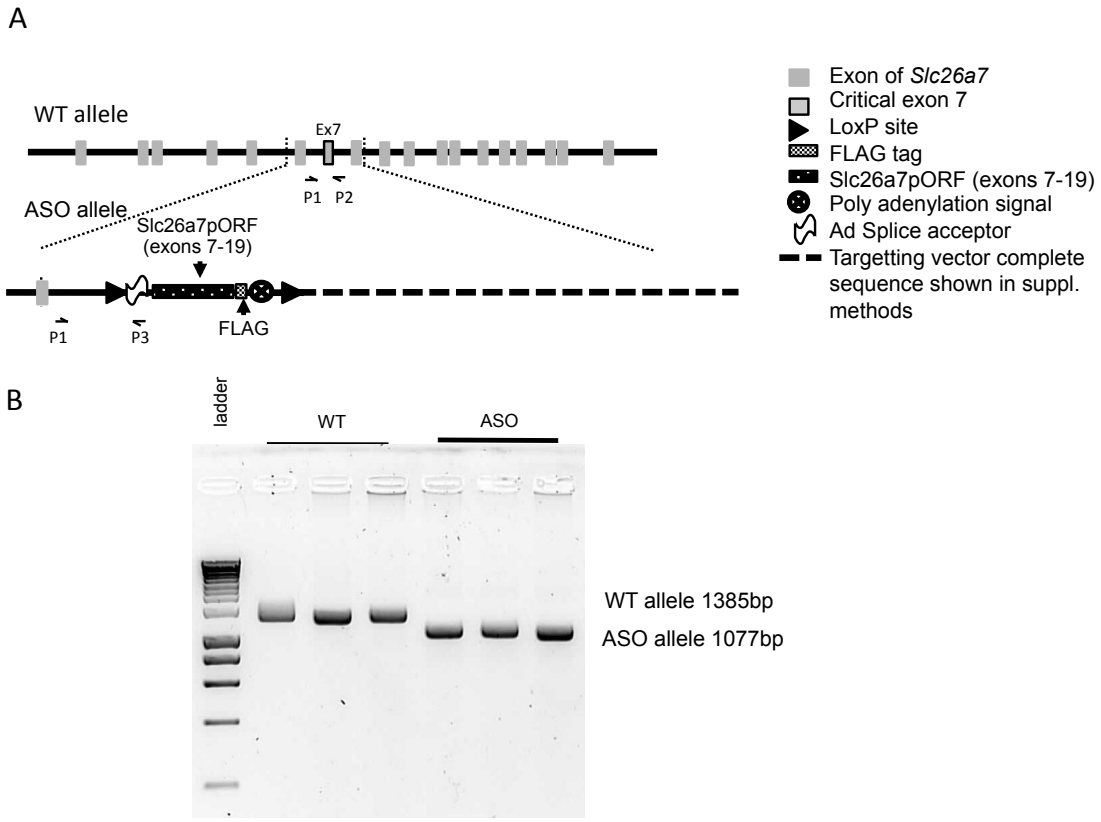

A. Schematic of the targeted locus in ASO mice expressing FLAG-Slc26a7 (more details shown in the supplementary methods section). Recognition sites for Cre recombinase (loxP black triangle); Slc26a7 critical exon 7 (grey rectangle); Ad Splice acceptor - Adenovirus splice acceptor site, pORF- cDNA corresponding to Slc26a7 exon 7 to 19, FLAG tag - FLAG sequence. The pORF feature allows the expression of FLAG tagged version of SLC26A7. B. Gel electrophoretic analysis of representative PCR amplifications from ASO and wild-type (WT) mice using the primers shown (P1, P2 WT allele, P1, P3 ASO allele). ASO mice used for immunostaining were homozygous for the ASO allele, detected as a 1077bp band using primers P1 and P3, compared with a 1385bp band for the WT allele, amplified using primers P1 and P2. Representative genotyping data is shown from three WT mice and three homozygous ASO mice. Ladder - HyperLadder 1kb (Bioline)

Supplementary Figure 3: Measurement of cellular iodide uptake in transfected HEK293 cells expressing ion transporters (A) and assessment of response to iodide supplementation in heterozygous and null male Slc26a7 mice (B-F)

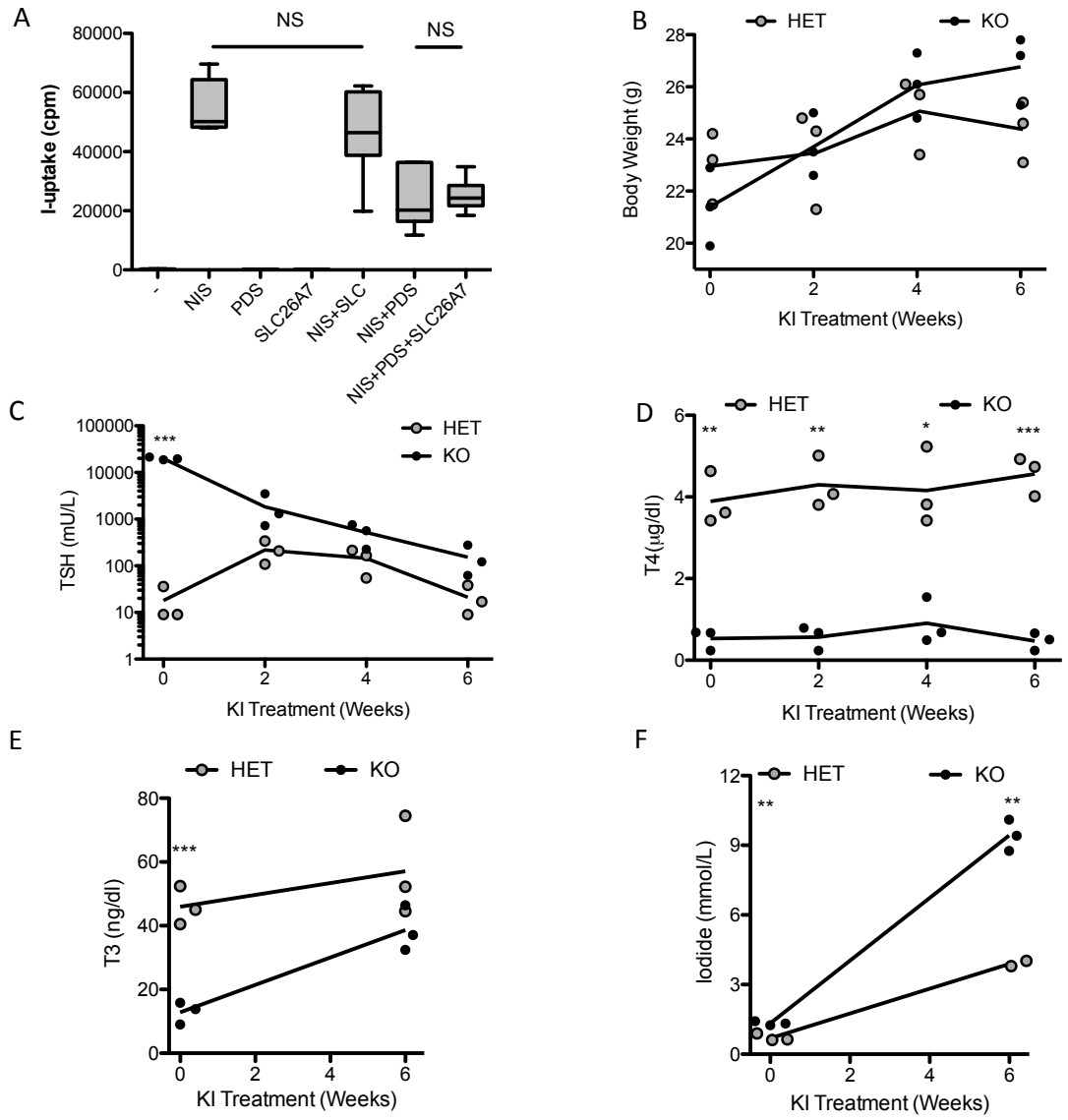

A. Box and whisker plots of iodide uptake in HEK293 cells transfected with empty vector (-), NIS, Pendrin (PDS), SLC26A7 alone or in combination. P values were calculated using one way ANOVA ($p=0.0001$) with Tukey's post hoc test to evaluate the effect of SLC26A7. Boxes extend from the 25th to 75th percentiles, the horizontal line represents the median and the vertical bars represent the minimum and maximum values. B-F. Response to 6 weeks iodide supplementation in 3 Slc26a7 null mice (black) and 3 Slc26a7 heterozygous euthyroid mice (grey) as controls: mice body weight (B), Serum TSH(C), T_4(D), T_3(E) and iodide(F) concentrations in heterozygous and Slc26a7 null mice at baseline and after iodide supplementation. Lines represent the mean for each group. P values were calculated using an unpaired, 2-tailed Student's T test. * $P<0.05$, ** $P<0.005$, *** $P<0.0005$, NS not significant.

Supplementary Table 2: Thyroid Biochemistry in cases with Heterozygous *SLC26A7* mutations

Case	AI.i	AII.ii	AII.vii	AII.ix	BI.ii	BI.i	CIi**	CIii**	DI.i	DI.ii	EI.i	EI,ii	F1.i	FI,ii
Age	32.8	12.3	4.3	2.8	46	32	34	28	48	45	45	42	29*	40++
TSH (mU/L)	0.96 (0.5-5.0)	1.97 (0.6-4.8)	2.1 (0.4-3.5)	1.97 (0.4-3.5)	1.37 (0.5-5.0)	2.86 (0.5-5.0)	1.69 (0.27-4.2)	2.87 (0.27-4.2)	**6.68** (0.3-4.2)	0.89 (0.4-6)	1.31 (0.4-6)	1.38 (0.3-4.2)	NA	NA
FT4 (ng/dl)	0.91 (0.7-1.6)	1.02 (0.76-1.5)	1.33 (0.83-1.7)	1.26 (0.83-1.7)	1.16 (0.7-1.6)	1.09 (0.7-1.6)	1.16 (0.93-1.7)	1.12 (0.93-1.7)	0.91 (0.85-1.7)	NA	1.03 (0.62-1.9)	1.20 (0.85-1.7)	NA	NA
FT3 (ng/dl)	NA	NA	NA	NA	0.44 (0.18-0.4)	0.37 (0.18-0.4)	0.29 (0.2-0.44)	0.28 (0.2-0.44)	NA	NA	NA	NA	NA	NA
Goiter	Nil	Nil	Nil	Nil	Nil	Nil	Nil	Nil	Nil	Nil	Nil	Nil	Nil	Nil

*has autoimmune hypothyroidism and thyroxine treatment (positive TPO AB) diagnosed at age of 29.
**Assumed heterozygous for *SLC26A7* mutation
++no symptoms or history of thyroid disease, TSH and T4 normal aged 39 years
FT3: multiply by 15.4 to convert to pmol/L, FT4: multiply by 12.87 to convert to pmol/L

Supplementary Table 3: Renal Biochemistry in cases with Homozygous *SLC26A7* mutations

Case	AII.i	AII.iii	AII.iv	AII.v	BII.i	CII.i	CII.ii	DII.i	EII.i	EII.ii	FII.i	FII.ii
Age	12.7	9.3	8.1	8.1	3	5.7	1.6	20.1	16.2	12.5	4.2	7.3
Na+ (mmol/L)	137	138	137	137	139	139	140	N	141	142	138	137
K+ (mmol/L)	3.7	4.0	3.6	3.7	4.3	4.7	5.0	N	3.9	3.9	4.1	3.9
Urea (mmol/L)	2.9	3.7	3.6	3.8	5.7	4.0	3.7	NA	NA	NA	NA	NA
Creatinine (μmol/L)	43	36	36	36	24	46	37	45	56	45	34	36
Cl- (mmol/L)	103	104	101	102	107	102	107	NA	105	104	NA	NA
Lactate (mmol/L)	NA	NA	NA	NA	NA	NA	NA	NA	1.65	NA	2.47	NA
Venous CO_2	26.1	25.6	25.7	25.3	23.6	39.4	43	42.8[A]	46.5[A]	44.3[A]	37.5[A,B]	40.5[A, B]
Venous HCO_3 (mEq/L)	NA	NA	NA	NA	NA	24.2	25.2	25	22	25	21.8[B]	22.7[B]
Venous BE	NA	NA	NA	NA	NA	-0.5	0	0.8	-1.5	0.1	-2.1	-1.4
Venous pH	NA	NA	NA	NA	NA	NA	NA	7.39	7.34	7.37	7.39	7.38
Urine pH	7.35	6.55	6.53	6.61	6.96	7.15	NA	7.25	NA	6.0	7.0	7.0

[A]Note Venous CO_2 is recorded in mEq/L for kindreds A and B, and mmHg for kindreds C-F, [B]Struggling during sampling.

Normal Ranges :

Na^+ (mEq/L): kindreds A, B 133-146; C 136-145; E, F 137-144

K^+ (mEq/L): kindreds A, B 3.5-5.0, C 3.5-5.1, E F: 3.4-4.7

Urea (mmol/L): kindreds A, B 2.5-6.5, C 1.7-8.3

Creatinine (μmol/L): kindreds A, B 32-55, C 17.7-70.7, D,EII.i 27-62; EII.ii:, F <63

Cl^- (mmol/L): kindreds A, B 95-108; C: 98-107, E: 96-111

Lactate (mmol/L) 0.6-2.0

Venous CO_2: kindreds A, B 19-28 mmol/L; C 35-45 mmol/L; D 30-50 mmHg; E, F 42-55 mmHg

Venous HCO_3 (mEq/L): kindreds C: 22-27; D, E, F: 24-28

Venous BE (mEq/L) -2.5 to +2.5